# SOL power decay length correlations with electron pressure pedestal top and pedestal gradients across L, I and H-modes at ASDEX Upgrade

D. Silvagni[1,2], T. Eich[1], M. Faitsch[1], T. Happel[1], B. Sieglin[1], P. David[1], D. Nille[1], L. Gil[3], U. Stroth[1,2], the ASDEX Upgrade team and the EUROfusion MST1 team[4]

[1]*Max-Planck-Institut für Plasmaphysik, Boltzmannstr. 2, 85748 Garching, Germany*
[2]*Physik-Department E28, Technische Universität München, 85748 Garching, Germany*
[3]*Instituto de Plasmas e Fusão Nuclear, Instituto Superior Técnico, Universidade Lisboa, PT*
[4]*see the author list "B. Labit et al. 2019 Nucl. Fusion accepted"*

## Introduction

Understanding how the scrape-off layer (SOL) power decay length $\lambda_q$ scales with plasma quantities is essential for designing fusion reactors and developing a power exhaust solution. Even though in the last years some progresses have been made in fundamental understanding of what sets the power fall-off length [1], it still remains an empirical science governed by scaling laws. To this respect, a major effort was done in 2011 in assembling a multi-machine database of inter-ELM H-mode power decay lengths in attached conditions [2]. It was shown that $\lambda_q$ scales approximately inversely with the poloidal magnetic field at the outer midplane and that such scaling is independent of machine size. More recently a new attempt in finding a cross-regime (L, I and H-mode) $\lambda_q$ dependence was carried out at Alcator C-mod [3]. It was found that the power decay length exhibits a dependence on volume-averaged core plasma pressure across all confinement regimes analyzed.
This paper investigates whether also local egde plasma parameters can describe the scaling of $\lambda_q$. To this end plasma phases in L-modes, I-modes, inter-ELM H-modes and the new ELM-free H-mode [4] recently discovered at ASDEX Upgrade (AUG) are analyzed. In addition, evidence of a correlation between SOL and pedestal electron pressure gradients is shown, which is in line with a critical-gradient transport paradigm governing the edge physics, as proposed in [5].

## Database and analysis technique

A broad database of different confinement regimes (L, I and H-modes), with different divertor geometries (closed divertor vs open divertor), different ion drift directions (ion $B \times \nabla B$ drift pointing to and away from the active X-point) and at different plasma conditions (density, temperature, plasma current etc.) is analyzed. All discharges analyzed are fuelled with deuterium. The heat flux onto the divertor targets is inferred from measurements obtained with infrared (IR) cameras [6]. They measure the divertor target surface temperature from which the heat flux is calculated using the implicit version [7] of the THEODOR code [8]. Heat flux profiles onto the divertor are fit with [9]:

$$q(\bar{s}) = \frac{q_0}{2}\exp\left[\left(\frac{S}{2\lambda_q}\right)^2 - \frac{\bar{s}}{\lambda_q f_x}\right]\operatorname{erfc}\left(\frac{S}{2\lambda_q} - \frac{\bar{s}}{S f_x}\right) + q_{\mathrm{BG}}, \tag{1}$$

where $\bar{s} = s - s_0$, $s$ is the location on target, $s_0$ is the strike line location, $\lambda_q$ is the power decay length mapped to the outer midplane via the flux expansion $f_x$, $S$ is the power broadening also mapped to the outer midplane and $q_{\mathrm{BG}}$ is the background heat flux. In order to evaluate $\lambda_q$ and $S$ within a certain time window, the following method is carried out. First, the fitting function is applied to each heat flux profile within the time window. Second, only pairs of $\lambda_q$ and $S$ satisfying the condition $\lambda_q/S \geq 1.5$ are taken into account. This condition is chosen because when $\lambda_q \simeq S$, the $\lambda_q$ measured at the divertor target is strongly influenced by the Gaussian broadening taking place in the divertor chamber, making any mapping to the outer midplane

more challenging. Last, the median of all the $\lambda_q$ (and $S$) values within the time window is calculated. The other important plasma quantity used in this work is the SOL electron pressure decay length. At ASDEX Upgrade SOL electron temperature and density profiles (from which the pressure can be obtained) are measured by a vertical Thomson scattering system [10]. The separatrix temperature is evaluated assuming electron conduction being the dominant parallel heat transfer process in the SOL. Following the approach in [11], $T_e^{\mathrm{sep}}$ can be estimated with the knowledge of both the power crossing the separatrix and $\lambda_q$ (and other plasma quantities such as $q_{\mathrm{cyl}}$, aspect ratio, elongation etc.). Once $T_e^{\mathrm{sep}}$ is known, the separatrix position ($r_{\mathrm{sep}}$) can be estimated and a subset of selected data (between $r_{\mathrm{sep}}-5$ mm and $r_{\mathrm{sep}}+9$ mm) is fit with an exponential, i.e. $T_e(r) = T_e^{\mathrm{sep}}\exp(-\frac{r-r_{\mathrm{sep}}}{\lambda_{T_e}})$, to find the SOL electron temperature decay length. An identical approach is used to evaluate the SOL electron density decay length. In order to have a more robust ensemble of datapoints to minimize fitting errors, several TS profiles within a long time window ($\approx 300$ ms) are collected before carrying out the fit.

**Scaling of the SOL power decay length**

The left panel of figure 1 shows the SOL power fall-off length mapped to the outer mid-plane against the volume-averaged plasma pressure defined as $\overline{p} = \frac{2}{3}W_{\mathrm{MHD}}/V$, where $W_{\mathrm{MHD}}$ is the plasma stored energy determined from the reconstructed magnetic equilibrium and $V$ is the plasma volume. For comparison the scaling found at Alcator C-mod ($\lambda_q = 0.91 \times (\overline{p}\ [\mathrm{atm}]\ )^{-0.48}$) is plotted in green. $\lambda_q$ shows a correlation with $\overline{p}$ but not with the same coefficient and expo-

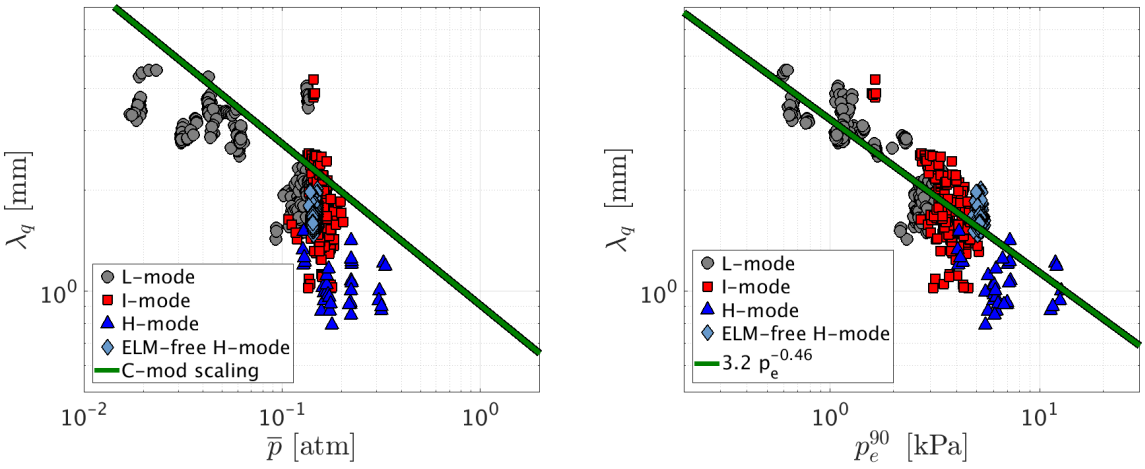


Figure 1: Power decay length $\lambda_q$ against the volume-averaged plasma pressure (left) and pedestal electron pressure (right). L-modes, I-modes, inter-ELM H-modes and ELM-free H-modes are represented in grey circles, red squares, blue triangles and light blue diamonds, respectively.

nent as in the C-mod scaling. In addition, for a volume-averaged plasma pressure of 0.15 atm (about 15 kPa) the data show a large scatter, i.e. $\lambda_q = [0.9;4]$ mm. In contrast, $\lambda_q$ data exhibit a clear alignment when plotted against the electron pressure pedestal top values, $p_e^{90}$ (evaluated at $\rho_{pol} = 0.90$), see right graph of figure 1. The correlation appears comparing all confinement regimes analyzed and results in a scaling with the inverse square root of $p_e^{90}$: $\lambda_q = 3.2 \times (\, p_e^{90}\,[\mathrm{kPa}]\,)^{-0.46}$. This result resembles the scaling found at Alcator C-mod which shows always an inverse square root dependence but with another quantity - the volume-averaged plasma pressure. However, at ASDEX-Upgrade the pedestal top electron pressure is found to be a more suitable and robust parameter for a $\lambda_q$ scaling. Indeed, $p_e^{90}$ is an edge local plasma

quantity that could be more related to the SOL physics setting $\lambda_q$ than a global quantity such as $\overline{p}$.

**On the connection between SOL and pedestal gradients**

To further investigate the reasons for the $\lambda_q$ inverse square root dependence with $p_e^{90}$, it is of interest to study the $\lambda_q$ relation with edge and SOL electron pressure gradients. The left graph of figure 2 shows the relation between the inverse of $\lambda_q$ and the pedestal electron pressure gradient $1/\lambda_{p_e}^{\text{ped}}$, which is estimated by: $\frac{1}{\lambda_{p_e}^{\text{ped}}} = \frac{p_e^{95}-p_e^{\text{sep}}}{R^{\text{sep}}-R^{95}} \cdot \frac{2}{p_e^{95}+p_e^{\text{sep}}}$, where the subscripts 'sep' and '95' denote values taken at the separatrix and $\rho_{\text{pol}} = 0.95$, respectively. The SOL power gradient and the electron pressure pedestal gradient are linearly correlated, even though with a larger scatter for I-mode discharges. In other words, it seems that an increase of the pedestal performance (i.e. steeper pedestal) is statistically associated with a steepening of the SOL power gradients (i.e. smaller $\lambda_q$). This observation sheds light on the chain of correlations which is ultimately leading

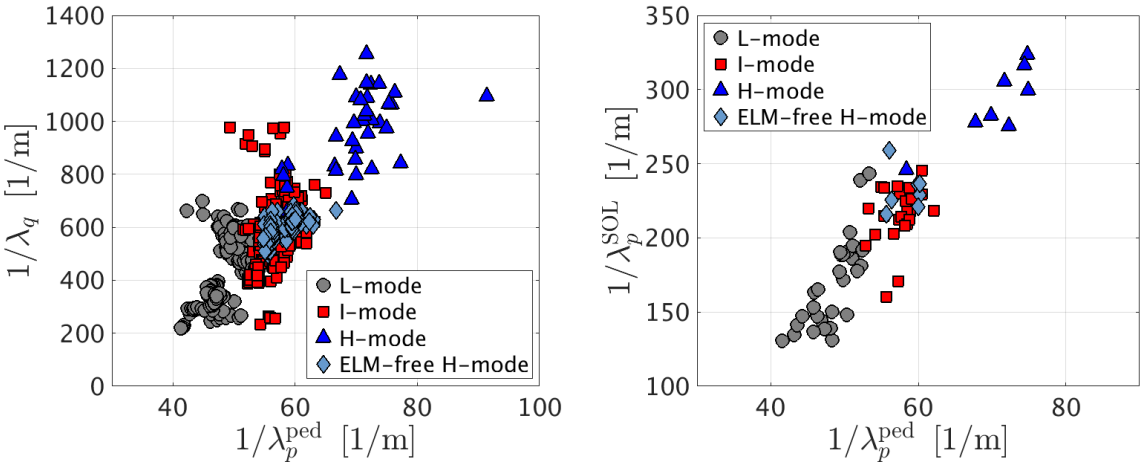


Figure 2: Left: SOL power gradient $1/\lambda_q$ against pedestal electron pressure gradient. Right: SOL electron pressure gradient against the pedestal electron pressure gradient. L-modes, I-modes, inter-ELM H-modes and ELM-free H-modes are represented in grey circles, red squares, blue triangles and light blue diamonds, respectively.

to the $\lambda_q$ scaling with the inverse square root of $p_e^{90}$: $\lambda_q$ is directly correlated with $\lambda_{p_e}^{\text{ped}}$, which is ultimately setting the electron pressure pedestal top value, if the pedestal width is not largely changing. This may be also the explanation behind the Alcator C-mod scaling, since there also a correlation between $\lambda_q$, electron pressure edge gradients and the pedestal pressure evolution is observed [12]. The right graph of figure 2 shows the relation between the SOL electron pressure gradient and the pedestal electron pressure gradient. Remarkably, SOL and pedestal gradients appear to be linearly correlated across all confinement regimes. This observation is in line with what suggested by LaBombard et al., namely that edge pressure gradients appear to be set by a critical-gradient transport paradigm (determined by electromagnetic fluid drift turbulence), rather than a classical diffusive-like transport [5, 12]. In other words, edge electron pressure gradients adjust themselves to satisfy marginal stability constraints and are linked to the near-SOL, as it sets the level of particle and heat input that is required to reach the desired plasma conditions just inside the last closed flux surface [5].

**Conclusions**

Among all the plasma quantities of the confined region, $\lambda_q$ exhibits its best correlation with the electron pressure evaluated at $\rho = 0.9$, $p_e^{90}$. In particular, data cluster around the scaling:

$\lambda_q = 3.2 \times (\, p_e^{90}\,[\mathrm{kPa}]\,)^{-0.46}$. This relation is highlighting that an increase of pedestal performances (i.e. larger $p_e^{90}$) is statistically associated with a reduction of $\lambda_q$. This, if confirmed also in detached plasmas, will have the consequence of reducing the operational windows of future next step devices [13], since the ultimate goal of a fusion power plant is to combine large core plasma pressure (which means high pressure pedestals) with a good enough power exhaust solution, which largely depends on a broad $\lambda_q$. In addition, it is shown that $\lambda_q$ exhibits a clear linear correlation with the pedestal electron pressure gradient. This explains the chain of correlations behind the $\lambda_q$ scaling with $p_e^{90}$: $\lambda_q$ relates with the pedestal electron pressure gradient, which is in turn setting the electron pressure at $\rho = 0.9$. The last and important observation is the one linking SOL and pedestal electron pressure gradients, which appear to be clearly correlated to each other across all confinement regimes. This is in line with what suggested in [5, 12], namely that edge pressure gradients appear to be set by a critical-gradient (determined by electromagnetic fluid drift turbulence), rather than a classical diffusive-like transport; in short, edge electron pressure gradients adjust themselves to satisfy marginal stability constraints. In such a picture, the near-SOL is responsible for setting the level of particle and heat input that is required to reach the desired plasma conditions just inside the separatrix [5]. This interpretation links near-SOL and pedestal electron pressure gradients and it could be a key ingredient to take into account for predicting $\lambda_q$.

## Acknowledgements

This work has been carried out within the framework of the EUROfusion Consortium and has received funding from the Euratom research and training programme 2014-2018 and 2019-2020 under grant agreement No 633053. The views and opinions expressed herein do not necessarily reflect those of the European Commission.

## References

[1] CHANG, C. S. et al., Nuclear Fusion **57** (2017) 116023.
[2] EICH, T. et al., Nuclear Fusion **53** (2013) 093031.
[3] BRUNNER, D. et al., Nuclear Fusion **58** (2018) 094002.
[4] GIL, L. et al., 45th European Physical Society Conference on Plasma Physics (2019).
[5] LABOMBARD, B. et al., Nuclear Fusion **45** (2005) 1658.
[6] SIEGLIN, B. et al., Review of Scientific Instruments **86** (2015) 113502.
[7] NILLE, D. et al., Bayesian Inference and Maximum Entropy Methods in Science and Engineering (2018).
[8] HERRMANN, A. et al., Plasma Physics and Controlled Fusion **37** (1995) 17.
[9] EICH, T. et al., Phys. Rev. Lett. **107** (2011) 215001.
[10] KURZAN, B. and MURMANN, H. D., Review of Scientific Instruments **82** (2011) 103501.
[11] EICH, T. et al., Nuclear Fusion **58** (2018) 034001.
[12] LABOMBARD, B. et al., Physics of Plasmas **18** (2011) 056104.
[13] KUKUSHKIN, A. et al., Journal of Nuclear Materials **438** (2013) S203 .